Article

Current Biology

A Perceptual Inference Mechanism for Hallucinations Linked to Striatal Dopamine

Highlights

- Auditory hallucinations are linked to a perceptual bias toward uncertain expectations
- Elevated striatal dopamine function relates to the same pattern of perceptual bias
- Volume of dorsal anterior cingulate relates to the same pattern of perceptual bias

Authors

Clifford M. Cassidy, Peter D. Balsam, Jodi J. Weinstein, ..., Nathaniel D. Daw, Anissa Abi-Dargham, Guillermo Horga

Correspondence

horgag@nyspi.columbia.edu

In Brief

Cassidy et al. induced auditory illusions to test a dopamine-dependent cognitive mechanism for hallucinations. Unmedicated schizophrenia patients with auditory hallucinations perceived tone durations in a way similar to what was expected, even when expectations were imprecise, and this perceptual bias related to excess dopamine function.

Cassidy et al., 2018, Current Biology *28*, 503–514
February 19, 2018
https://doi.org/10.1016/j.cub.2017.12.059

CellPress

Current Biology
Article

A Perceptual Inference Mechanism for Hallucinations Linked to Striatal Dopamine

Clifford M. Cassidy,[1,2] Peter D. Balsam,[1,3] Jodi J. Weinstein,[1,4] Rachel J. Rosengard,[1] Mark Slifstein,[4] Nathaniel D. Daw,[5] Anissa Abi-Dargham,[1,4] and Guillermo Horga[1,6,*]
[1]Department of Psychiatry, New York State Psychiatric Institute, Columbia University Medical Center, 1051 Riverside Drive, New York, NY 10032, USA
[2]The Royal's Institute of Mental Health Research, University of Ottawa, 1145 Carling Avenue, Ottawa, ON K1Z 7K4, Canada
[3]Department of Psychology, Columbia University, 3009 Broadway, New York, NY 10027, USA
[4]Department of Psychiatry, Stony Brook University, 100 Nicholls Road, Stony Brook, NY 11794, USA
[5]Department of Psychology, Princeton University, South Drive, Princeton, NJ 08540, USA
[6]Lead Contact
*Correspondence: horgag@nyspi.columbia.edu
https://doi.org/10.1016/j.cub.2017.12.059

SUMMARY

Hallucinations, a cardinal feature of psychotic disorders such as schizophrenia, are known to depend on excessive striatal dopamine. However, an underlying cognitive mechanism linking dopamine dysregulation and the experience of hallucinatory percepts remains elusive. Bayesian models explain perception as an optimal combination of prior expectations and new sensory evidence, where perceptual distortions such as illusions and hallucinations may occur if prior expectations are afforded excessive weight. Such excessive weight of prior expectations, in turn, could stem from a gain-control process controlled by neuromodulators such as dopamine. To test for such a dopamine-dependent gain-control mechanism of hallucinations, we studied unmedicated patients with schizophrenia with varying degrees of hallucination severity and healthy individuals using molecular imaging with a pharmacological manipulation of dopamine, structural imaging, and a novel task designed to measure illusory changes in the perceived duration of auditory stimuli under different levels of uncertainty. Hallucinations correlated with a perceptual bias, reflecting disproportional gain on expectations under uncertainty. This bias could be pharmacologically induced by amphetamine, strongly correlated with striatal dopamine release, and related to cortical volume of the dorsal anterior cingulate, a brain region involved in tracking environmental uncertainty. These findings outline a novel dopamine-dependent mechanism for perceptual modulation in physiological conditions and further suggest that this mechanism may confer vulnerability to hallucinations in hyper-dopaminergic states underlying psychosis.

INTRODUCTION

Perception is an inherently subjective process that is biased by beliefs acquired through experience [1]. Whereas these biases can adaptively facilitate disambiguation of noisy sensory stimuli, they can also confer a predisposition to perceptual distortions (for instance, the common perception of a cell phone vibrating in the pocket in the absence of true vibration) [2]. Patients with schizophrenia often experience extreme and maladaptive perceptual disturbances such as hearing voices in the absence of true speech stimuli. Such auditory hallucinations and other cardinal psychotic symptoms respond to antidopaminergic treatment [3], worsen with prodopaminergic drugs [4, 5], and their severity—beyond a categorical diagnosis of schizophrenia—correlates with excessive dopamine release in the associative striatum [6, 7]. However, the mechanism through which dopamine excess leads to hallucinations remains unknown [8].

Beyond their role in reinforcement learning [9–11], neuromodulators, including dopamine, have been proposed to contribute to experience-dependent sensory learning [12–14]. Specifically, Bayesian models posit that perception results from an optimal integration of bottom-up sensory evidence and top-down sensory predictions or priors [15]. Such integration depends on the precision of these top-down sensory predictions (mathematically defined as the inverse of the variance of the prior and more intuitively related to the confidence or certainty of expectations) [15–18], a key variable thought to be encoded by neuromodulators such as dopamine [18]. Under this Bayesian framework (Figures 1D and 1E), perceptual biases toward context-dependent predictions may explain sensory illusions [19, 20] and, in extreme cases, hallucinatory percepts [21, 22]: dopamine dysregulation could lead to faulty signaling of the precision of predictions, with systematic overconfidence in the predictions resulting in disproportionate perceptual biases toward expected states [17, 18, 23]. Importantly, under this model of hallucinations [17, 23–25], perceptual biases in psychosis would be even more apparent in highly uncertain contexts (i.e., in situations that should normally lead to imprecise predictions and hence weaker top-down predictions), an assumption that remains to be tested. Note that, according to some models, this pattern of

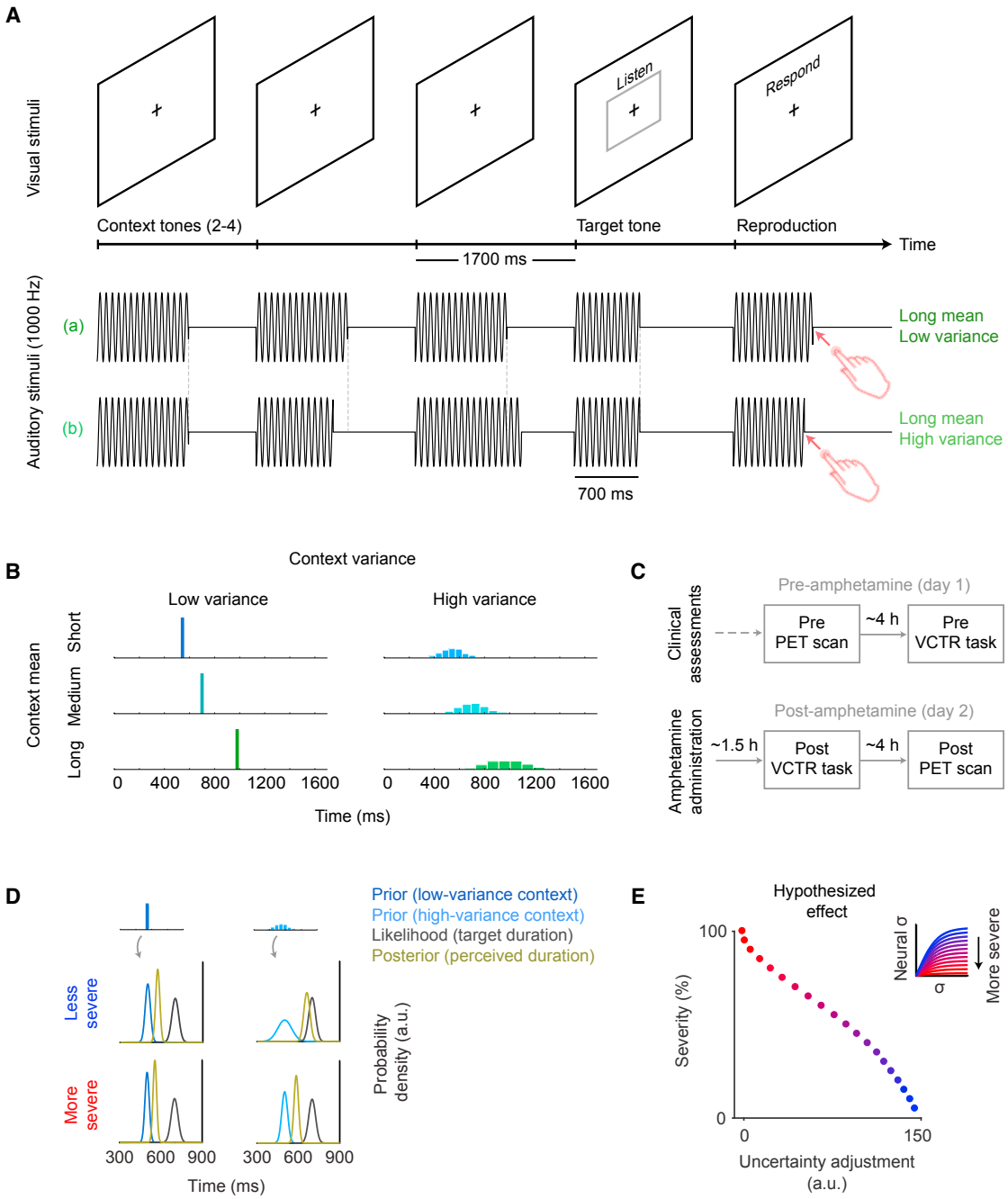

Figure 1. Experimental Design and Theoretical Model of Hallucinations

(A) Schematic of the variable context tone reproduction (VCTR) task structure. Representative trials are shown depicting auditory stimuli in different conditions (with long context mean and low [a] or high [b] variance) followed by the reproduction procedure used to match the perceived duration of the target tone. The target stimulus is held constant (at 700 ms) in 90% of the trials whereas the context randomly varies in mean duration (context mean), duration variability across tones (context variance), and number of tones (context length).

(B) Magnitude and distribution of context tone duration within a trial, showing histograms of context mean and context variance under all experimental conditions (comprising a 3 × 2 parametric design).

(C) Flow chart of experimental procedures in study 2.

(D) Hypothesized effects of context variance under a model of Bayesian inference and hallucinations (see Model description and simulations in STAR Methods). Four panels show short context-mean trials in the VCTR task for the two context variance conditions (low and high from left to right, respectively) in less severe and more severe pathological conditions (top and bottom, respectively). The target stimulus, as in the VCTR task, is kept constant, thus leading to equivalent sensory evidence (likelihood) in all four cases. The precision of the prior (the width of the prior distribution rather than its expected mean value) depends on context variance and thus determines the relative weighting of prior and likelihood and the ensuing percept (posterior). In the less severe condition (top panels, representing non-hallucinating patients), the high-variance context (right) leads to a more imprecise prior with a lesser effect on perception toward contextual

(legend continued on next page)

bias would only be present during the psychotic state, and individuals with schizophrenia could otherwise exhibit *weak* top-down predictions [18], whereas other models make the opposite prediction that weak top-down predictions could even underlie hallucinations [26].

Here, we developed a novel auditory interval-reproduction paradigm—the variable context tone reproduction (VCTR) task—that induces an auditory illusion whereby the perceived duration of a 700-ms target tone is modulated by a preceding train of context tones. Context tones differ systematically in their mean duration (context mean) and variability (context variance) to target the main components of Bayesian inference: predictions and their precision, respectively. This type of task is suitable to study processes dependent on dopamine and basal ganglia circuits [27–29] and to study Bayesian inference, as temporal perception is influenced by the distribution of previously experienced durations—often generating a perceptual bias toward the expected duration (assimilation) [30–32] (but under certain conditions [33] leading to the opposite effect [contrast] [34]). Furthermore, under normal conditions, the extent of this perceptual bias—the degree of assimilation—degrades when uncertainty of predictions is high (and precision low) [15, 17, 18], reflecting an uncertainty adjustment whereby predictions become less influential on perception under more uncertain contexts. In contrast, a failure to degrade this perceptual bias with high uncertainty of predictions would manifest as a reduced uncertainty adjustment, a pattern that would constitute a laboratory model supporting the candidate mechanism for hallucinations that we set out to test.

To investigate the computational mechanisms of hallucinations in schizophrenia and their relationship to striatal dopamine dysfunction, we obtained behavioral data with the VCTR task and a well-validated positron emission tomography (PET) measure of striatal dopamine before and after an amphetamine challenge, as well as structural magnetic resonance imaging (MRI) scans, in unmedicated patients with schizophrenia (to avoid confounds associated with dopamine receptor blockade) with varying degrees of hallucination severity and healthy controls.

RESULTS

Study 1: Uncertainty Effects on Perception in Health

Thirty subjects completed the study (see Table 1). In the duration-sensitivity task, in which tones were reproduced in the absence of context tones, subjects were able to accurately reproduce variation in tone duration over the range employed in the VCTR task ($t_{29} = 17.3$; $p < 10^{-16}$; one-sample t test of βs from subject-level regressions of actual tone duration against reproduction duration). Participants were able to maintain attention throughout the VCTR task: none missed a reproduction in more than 5 of the 120 trials, and on "catch" trials, when the target tone duration was actually different from 700 ms, subjects effectively tracked this variation throughout the experiment ($t_{29} = 14.3$; $p < 10^{-13}$; one-sample t test of βs from subject-level regressions of actual target tone duration against reproduction duration).

Effects of Context-Mean Duration and Uncertainty on Perception

As intended, the mean duration of context tones (context mean) influenced perception of the target tone (i.e., it induced an illusion or perceptual bias). For most subjects, the perceived duration of the target tone was closer to the context mean (assimilation bias; see Figure 2A). For a few subjects, it was instead further away from the context mean (contrast bias; Figure 2C). Thirteen out of 30 subjects (43.33%) showed a significant context-mean effect at $p < 0.05$ (9 were assimilators, 4 contrasters). A permutation test in which tone reproduction data were randomly shuffled with respect to context conditions (10,000 permutations) indicated that this was not merely due to chance, as only 4.7% of permuted subjects' data showed a significant context-mean effect (a significantly smaller proportion than in the real data; $\chi^2 = 97.39$; $p = 10^{-23}$). Context-mean β_1 values from real subjects also had a greater spread than those from permuted subjects ($F_{1,\ 10,028} = 34.5$; $p < 10^{-9}$; Levene's test; see Figures 2E and 2F). The coexistence of assimilation and contrast biases in our sample was also present in pilot data and did not appear to result from individuals with enhanced duration sensitivity being more prone to contrast biases [33, 34], as these variables were only weakly correlated ($r = -0.23$; $p = 0.23$). Thus, two separate mechanisms may account for the observed behavior, consistent with previous extended Bayesian models of perception (e.g., where anti-Bayesian or contrast biases may depend on increased sensory noise among other factors) [15, 35]; here, our *a priori* candidate mechanism for hallucinations was the Bayesian mechanism underlying perceptual assimilation and, in particular, its modulation by uncertainty.

Also as intended, context variance (i.e., variability in the duration of context tones) modulated the strength of the context-mean effect such that this effect was stronger in the low-variance condition than in the high-variance condition ($F_{1,58} = 7.30$; $p = 0.009$; Levene's test). This was true for subjects who showed an assimilation bias in the low-variance condition ($\beta_1 > 0$; assimilators; $n = 20$; $t_{19} = 4.40$; $p = 0.0003$; paired t test) and for those who showed a contrast bias in the low-variance condition ($\beta_1 < 0$;

assimilation (i.e., the posterior is closer to the likelihood than it is to the prior) compared to the low-variance context (left). We refer to this pattern as a (positive) uncertainty adjustment. In this implementation of the model, in the more severe condition (bottom panels, representing a more pathological state in hallucinating patients), the difference in precision of the priors for the high- and low-variance contexts is not as manifest as in the less severe condition: the precision of the prior is high even in the high-variance context (right) and thus percepts in both contexts are substantially influenced by the priors (i.e., the posterior is closer to the prior than it is to the likelihood in both contexts, which results in a more apparent difference between the more and less severe conditions in the high-variance context [top right versus bottom right]; in other words, the more severe condition is associated with a generalized increase in assimilation toward the context, leading to smaller differences between high- and low-variance contexts and reduced uncertainty adjustment).

(E) Simulation of VCTR task effects under a model of Bayesian perceptual inference in hallucinators. More severe pathology (i.e., more severe hallucination-related pathology in patients, indicated as a gradient from blue to red) is associated with reduced uncertainty adjustment in the VCTR task, measured as more assimilation (posterior closer to the prior) under the more uncertain (high-variance) relative to the less uncertain (low-variance) condition. The inset plot indicates the neural encoding of uncertainty; the estimated context variance, as encoded neurally (neural σ), is a function f(σ) of the true contextual uncertainty σ, which saturates earlier with more severe pathology (i.e., neural σ has a more restricted range with increasing severity).

Table 1. Sociodemographic, Clinical, and PET Data

	Study 1	Study 2		
	Healthy Individuals (n = 30)	Healthy Controls (n = 17)	Patients (n = 16)	Group Comparison p Value[a]
Sociodemographic Characteristics				
Gender (male)	15 (50%)	12 (70.6%)	10 (62.5%)	0.62
Age (years)	29.8 ± 9.2	29.5 ± 8.4	30.6 ± 11.6	0.75
Ethnicity (African American)	8 (26.7%)	7 (41%)	10 (63%)	0.22
Subject socioeconomic status	33.6 ± 12.0	40.9 ± 14.4	20.8 ± 6.9	<0.001
Parental socioeconomic status	45.5 ± 12.9	48.2 ± 9.5	42.1 ± 14.2	0.2
Clinical Characteristics				
Positive symptom severity (PANSS positive subscale score)	–	7.2 ± 0.4	16.5 ± 5.9	<0.001
Negative symptom severity (PANSS negative subscale score)	–	9.7 ± 2.8	17.4 ± 5.4	<0.001
MATRICS composite cognition score	–	42 ± 6.7	37.4 ± 10.7	0.33
Naive to antipsychotic medication	–	–	10 (63%)	–
PET Data				
Interval between oral amphetamine and PET scan (hours)	–	5.38 ± 0.95	5.36 ± 1.41	0.97
Plasma amphetamine level during PET scan (ng/mL)	–	73.8 ± 14.6	69.1 ± 10.3	0.46
Interval between oral amphetamine and VCTR task (minutes)	–	105 ± 9.8	100 ± 8.3	0.25
Injected radiotracer mass (pre-amphetamine scan, μg)	–	2.47 ± 2.12	1.86 ± 0.54	0.39
Injected radiotracer dose activity (pre-amphetamine scan, mCi)	–	8.0 ± 2.7	10.2 ± 2.9	0.12
Injected radiotracer mass (post-amphetamine scan, μg)	–	2.60 ± 1.28	2.00 ± 0.81	0.24
Injected radiotracer dose activity (post-amphetamine scan, mCi)	–	11.0 ± 2.7	10.8 ± 2.8	0.88

Means ± SD are given for continuous variables; number (and percentage) is given for categorical variables. PANSS, Positive and Negative Syndrome Scale (positive or psychotic symptoms of schizophrenia include hallucinations and delusions; negative symptoms include emotional withdrawal and amotivation); MATRICS, Measurement and Treatment Research to Improve Cognition in Schizophrenia (Consensus Cognitive Battery).
[a]p values for group comparison of unmedicated patients and healthy controls in study 2 are given based on two-sample t tests for continuous variables and X^2 tests for categorical variables.

contrasters; n = 10; $t_9 = -3.32$; p = 0.009; paired t test; see Figures 2B and 2D). This suggests that higher context variance led to higher uncertainty about expectations (a more imprecise prediction), degrading the contextual influence on perception. Again, the permutation test indicated that this observation was unlikely due to chance: the distribution of the context-mean β_1 values from the permuted subjects was similar in the low-variance (SD = 0.027) and high-variance conditions (SD = 0.027; $F_{1,\ 19{,}998} = 2.37$; p = 0.12; Levene's test).

For further analyses, the effect of uncertainty on perception was measured individually as the interaction of context mean × context variance on reproduction durations across trials (the weight of this interaction term, made negative to aid interpretation [$-\beta_3$], is referred to as a subject's uncertainty adjustment); these analyses controlled for the context-mean effect and thus for whether a subject was an assimilator or a contraster. Note that, for assimilators, a more positive (larger) uncertainty adjustment represents the normative behavior whereby the perceptual bias toward the expected tone duration under the low-variance condition is reduced under the high-variance condition—i.e., the assimilation bias is degraded with higher contextual variance. (Note that, for the few contraster subjects, in contrast, a larger uncertainty adjustment would instead represent a paradoxical effect whereby the perceptual bias away from the expected tone duration would be exaggerated with higher contextual variance.)

Alternative Explanations of the Data

To support our argument that the influence that context tones had on reproduction duration was in fact due to changes in perception and not to other factors, a control version of the VCTR task was developed (motor-control task). Unlike in the VCTR task itself, this control task showed no difference between real and randomly permuted data on context-mean effects ($F_{1,\ 10{,}008} = 0.18$; p = 0.67; Levene's test), suggesting that motor control was not influenced by the presence of context tones. Also consistent with our interpretation that context tones influenced perception, subjects had explicit knowledge of the illusions experienced during the VCTR (r = 0.36; p = 0.051; correlation between self-reported contrast-assimilation score and context-mean effect). Furthermore, the context-mean effect and uncertainty adjustment were unrelated to cognitive performance, working memory, sleep quality, or most general accuracy measures (all $r < |0.3|$; $p > 0.05$). The exception was the "catch" trial effect, which was negatively correlated to the context-mean effect (r = −0.43; p = 0.017), consistent with the notion that assimilators weigh sensory evidence less strongly. Finally, an alternative, non-Bayesian model was considered in which only the last tone in a context train affected

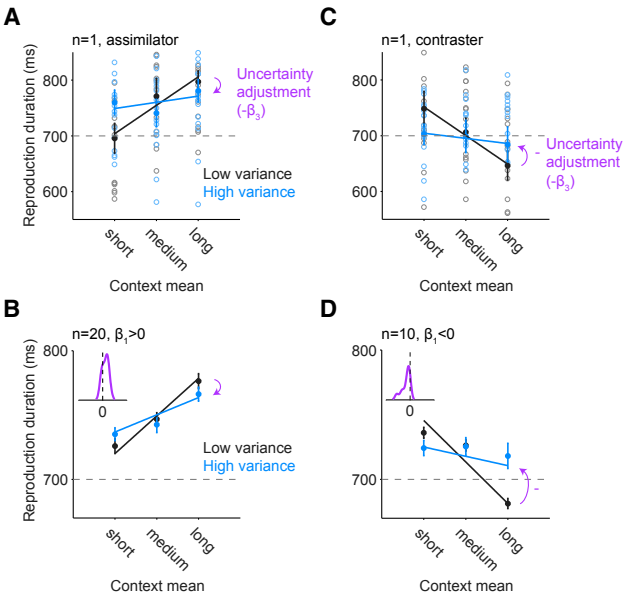

Figure 2. Uncertainty-Dependent Modulation of Perception in Health

(A and C) Representative single subjects' data are shown. Empty circles are reproduction durations from single trials following short, medium, or long contexts (x axis) with low (blue) or high (black) variance. Filled circles are the average reproduction duration for each condition; error bars are SEM. For each subject, the slope of the black line represents the context-mean effect and the difference in slopes (blue minus black) represents the uncertainty adjustment. The magenta arrows indicate the sign of the uncertainty adjustment. Note that the subject in (A) has a positive slope in the low-variance condition and is therefore an assimilator, whereas the subject in (C) has a negative slope and is therefore a contraster.

(B and D) Group average reproduction times are shown as filled circles both for the group of assimilators (B) and contrasters (D) by context condition. Error bars are the SEM, mean centered for each subject in each context variance condition. The lines reflect the fitted regression line across subjects. The distribution of the uncertainty adjustment is shown by inset magenta histograms with kernel smoothing function fits in the group of assimilators (B) and contrasters (D).

(E and F) Distribution of context-mean effect β in the real data (E) and permuted data in which the context condition labels were randomly shuffled with respect to reproduction durations (F). Histograms consist of kernel smoothing function fits. Dotted lines indicate the top and bottom 10% of observed values. In the low-variance condition (black line), the context-mean effect shows a broader distribution with subjects having more extreme values in both the positive and negative direction than would be expected by chance according to the permuted data (10,000 permutations).

perception of the target (i.e., whereby subjects did not process information about context mean or uncertainty). Analyses did not support the inclusion of this "last-tone" variable as an independent predictor in models predicting reproduction durations (all $p > 0.1$; one-sample t test).

Relationship to Subthreshold Hallucination-like Phenomena in Healthy Individuals

The tendency to experience hallucination-like phenomena (Launay-Slade Hallucination Scale [LSHS] scores) in healthy individuals was not significantly related to uncertainty adjustment (Spearman's $\rho = -0.21$; $p = 0.26$) or the context-mean effect ($\rho = -0.14$; $p = 0.47$). When excluding contrasters, we still did not find a significant correlation between LSHS score and uncertainty adjustment ($\rho = -0.16$). The effect size of the relationship of uncertainty adjustment to hallucination-like phenomena in healthy controls was not significantly smaller than that of the relationship between uncertainty adjustment and hallucinations in patients with schizophrenia reported in study 2 below (comparison of correlations observed in studies 1 and 2; $z = 1.08$; $p = 0.14$).

Study 2: Relationship of Uncertainty Adjustment to Hallucination Severity, Dopamine, and Regional Brain Volume

Sixteen unmedicated patients with schizophrenia with varying degrees of hallucination severity (from not active [four patients] to mild-to-moderate [five patients] to moderate-severe-to-severe hallucinations [seven patients]) and 17 matched healthy controls completed study 2 (Table 1). Given our primary focus on the mechanisms of hallucinations (beyond schizophrenia as a diagnostic group), our primary analyses focused on the correlates of hallucination severity within the patient group. Simplifying the interpretation of the primary results within this group and despite the interindividual variability among healthy individuals in study 1, all patients with a significant context-mean effect exhibited an assimilation bias and none exhibited a significant contrast bias. Secondary analyses compared patients to the matched control group.

Relationship to Hallucination Severity in Schizophrenia

Consistent with our main *a priori* hypothesis, hallucination severity in patients correlated strongly with reduced uncertainty adjustment (Positive and Negative Syndrome Scale [PANSS]-P3 "hallucinations item" scores; Spearman $\rho = -0.70$; $p = 0.008$; partial correlation controlling for context-mean effect, positive symptom severity excluding hallucinations, and negative symptom severity; see Figure 3A). Hallucination severity also correlated positively with the context-mean effect ($\rho = 0.61$; $p = 0.028$; partial correlation controlling for uncertainty adjustment, positive symptom severity excluding hallucinations, and negative symptom severity). These findings suggest that assimilation biases tend to be stronger in more hallucination-prone patients and that assimilation biases also degrade to a lesser extent in uncertain contexts in these patients (i.e., they exhibit reduced uncertainty adjustment). The hallucination-related reduction in uncertainty adjustment was driven by a numerically stronger correlation between hallucination severity and the context-mean effect in the high-variance condition ($\rho = 0.54$; $p = 0.047$) compared to the low-variance condition ($\rho = 0.29$; $p = 0.31$; correlations controlled for other types of symptoms but not uncertainty adjustment; Figures 3B and 3C). The difference in the strength of these correlations did not reach statistical significance ($z = 1.43$; $p = 0.15$).

Although no patients showed significant contrast biases, even removing any patients with an effect in the direction of contrast

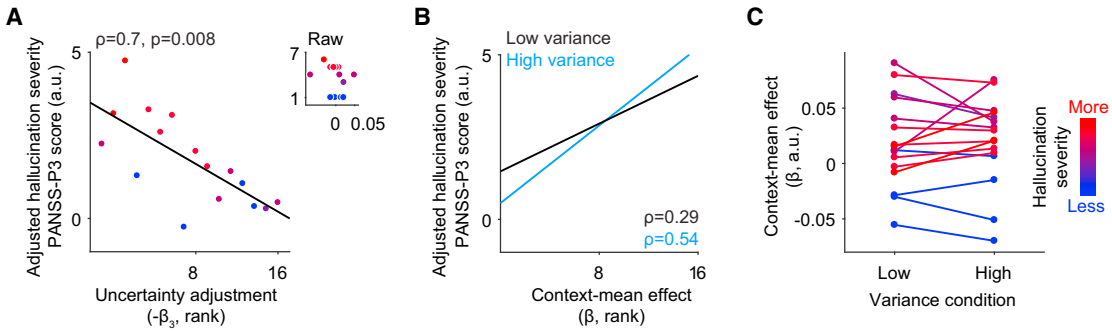

Figure 3. Relationship between Measures of Perceptual Bias and Hallucinations in Patients

(A) Scatterplot indicating the correlation between severity of hallucinations in patients with schizophrenia and uncertainty adjustment (or tendency to reduce assimilation biases under high contextual uncertainty). Hallucination severity was adjusted based on the other predictors in the model (see Results), and all variables were rank ordered. Data points are color coded according to hallucination severity (see color bar at far right). a.u., arbitrary units. The inset shows the same relationship with raw, unadjusted data plotted on both axes.

(B) Regression lines relating severity of hallucinations in patients with schizophrenia (adjusted based on other predictors in the model) to the context-mean effect at low (black) and high (blue) variance.

(C) Plot indicating the context-mean effect at the low- and high-variance conditions for each patient. The slope of the line connecting responses in the two conditions represents the uncertainty adjustment: here, more negative slopes represent more normative uncertainty adjustments, whereas less negative or more positive slopes represent reduced uncertainty adjustment. Each line is color coded according to the individual's hallucination severity. Note that hallucinators are perfectly separated from non-hallucinators based on the context-mean effect under high uncertainty (high variance).

See also Figure S1.

($\beta_1 < 0$; n = 5) had no meaningful impact on the results (uncertainty adjustment correlation to hallucination severity: $\rho = -0.60$). Critically, these effects were specific to hallucinations compared to other symptoms, because positive (excluding hallucinations), negative, and general PANSS subscale scores were uncorrelated with uncertainty adjustment or context-mean effect (all $\rho < |0.2|$), and the strength of the correlation of uncertainty adjustment to hallucination severity was significantly greater than its correlation to other positive symptoms ($z = 2.48$; $p = 0.013$). Unsigned measures of the context-mean effect and uncertainty adjustment (related to the strength of the illusion but independent of its direction toward assimilation or contrast) did not correlate with hallucination severity (all $\rho < |0.32|$), indicating it is not the absolute strength of the illusion that relates to hallucinations but its specific direction toward assimilation. General accuracy measures did not correlate with hallucination severity (all $\rho < |0.3|$).

Comparison to Healthy Controls

For comparison purposes, in exploratory analyses, we divided patients into those with active hallucinations and those without and compared them to controls. No group differences in general accuracy measures were found (all $p > 0.3$). Six controls (35.29%), 4 hallucinators (33.33%), and 0 non-hallucinators showed a significant context-mean effect (in the direction of assimilation for all of the hallucinators and half of the controls). There were no significant differences across groups in the proportion of assimilators ($p = 0.30$; Fisher's test), the context-mean effect ($F_{2,30} = 2.38$; $p = 0.11$), or the uncertainty adjustment ($F_{2,30} = 0.34$; $p = 0.71$; Figures S1B and S1A), but hallucinators numerically exhibited the strongest scores for both effects. Excluding contrasters did not affect the results of the group comparison on the uncertainty adjustment ($p = 0.9$). Considering the context-mean effect under high variance (the sum of the context-mean effect and its change with the introduction of uncertainty; $\beta_1 + \beta_3$), there was a significant difference across groups ($F_{2,29} = 4.91$; $p = 0.015$; Figure S1C) after removing one control, who was an influential outlier in this analysis (Cook's distance = 0.21; cut-off (4/n) = 0.12; studentized residual = 4.5; Bonferroni-corrected $p = 0.003$). Post hoc tests further provided preliminary support for greater assimilation in the high-variance condition in hallucinators compared to controls ($t_{26} = 2.11$; $p = 0.045$), although this difference would not survive a correction for multiple comparisons (3 comparisons). When pooling together patients with and without active hallucinations for completeness, we found that a diagnosis of schizophrenia was not itself associated with an abnormal uncertainty adjustment or context-mean effect (all $p > 0.4$).

Pharmacological Effects of Amphetamine

After finding that hallucination severity correlated most strongly with more negative (reduced) uncertainty adjustment, we tested in a subsample of 23 subjects (in study 2, 11 healthy individuals and 12 schizophrenia patients) whether pharmacologically stimulating dopamine release via amphetamine would induce this pattern. There was no main effect of amphetamine (pre- versus post-amphetamine sessions) on the uncertainty adjustment ($F_{1,21} = 1.9$; $p = 0.19$) and no diagnosis × amphetamine interaction ($p = 0.65$). However, this linear test would be inadequate if the uncertainty adjustment had a floor—i.e., a non-linearity like the well-documented non-linear relationship between dopamine and other cognitive processes [36–38]. Consistent with this possibility, we found that the amphetamine-induced change in uncertainty adjustment was greater for subjects with larger baseline uncertainty adjustment (robust linear regression; $\beta = 0.94$; $p = 0.006$). Thus, we controlled for baseline uncertainty adjustment (pre-amphetamine session) and found that the reduction in the uncertainty adjustment was significantly greater than zero in subjects with baseline uncertainty adjustment above the median (intercept $\beta = -0.034$; $p = 0.007$), but not in subjects

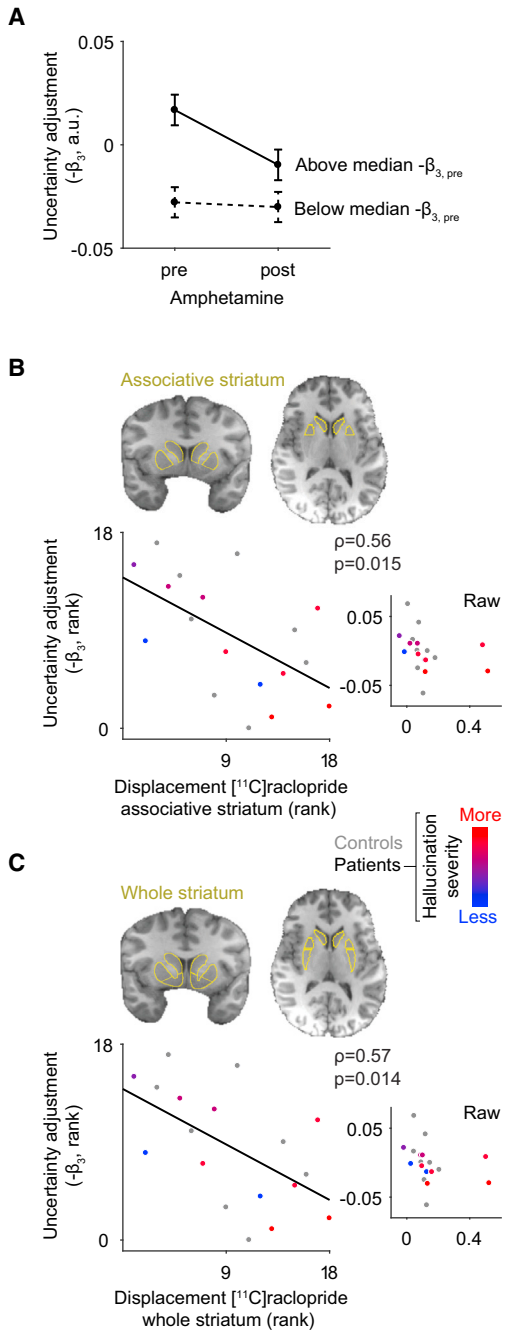

Figure 4. Relationship between Uncertainty Adjustment and Dopamine

(A) Changes in uncertainty adjustment following administration of amphetamine. Uncertainty adjustment before and after amphetamine is plotted for subjects above and below the median for the baseline (pre-amphetamine) uncertainty adjustment. Error bars represent SEM.

(B and C) Scatterplots show that subjects with higher striatal dopamine release capacity have significantly reduced uncertainty adjustment at baseline (pre-amphetamine condition). This is clear in the associative striatum (B; *a priori* region of interest [ROI]) and the whole striatum (C). The larger plot shows ranked data on both axes, and the inset plot shows the raw data for the same variables. The brains depict the manually traced striatal ROIs of a single subject overlaid on the subject's T1 anatomical MRI scan. a.u., arbitrary units. See also Table S1.

below the median (intercept β = 0.006; p = 0.56; robust linear regression of change in uncertainty adjustment versus baseline uncertainty adjustment, re-centered at baseline mean for each group). This suggests that amphetamine induced a reduction in the uncertainty adjustment but only in those subjects who had a large uncertainty adjustment at baseline, suggesting a non-linear floor effect whereby reduced uncertainty adjustment at baseline was not reduced further under amphetamine (Figure 4A). Note that the presence of this effect in only one group is inconsistent with regression to the mean. The amphetamine-induced reduction in uncertainty adjustment was still present for subjects with baseline uncertainty adjustment above the median when contrasters were excluded (intercept β = −0.038; p = 0.006; n = 21). No significant main effects or interactions were observed for the context-mean effect (all p > 0.4).

Relationship to Striatal Dopamine Release Capacity

Hallucination severity in patients (n = 10) correlated with greater dopamine release in the associative striatum (ρ = 0.74; p = 0.015), consistent with the known relationship between dopamine release capacity and psychosis severity [7]. Critically and consistent with our hypothesis, reduced uncertainty adjustment correlated with greater dopamine release capacity in the associative striatum (p = 0.015; patients and controls, n = 18; Figure 4B). This relationship was stronger in the associative striatum than in other striatal subregions (Table S1). The relationship held after controlling for the context-mean effect in all subjects (ρ = −0.50; p = 0.041), if contrasting subjects were removed (ρ = −0.56; p = 0.019; n = 17) and if participants were divided into patients (ρ = −0.71; p = 0.003) and healthy controls (ρ = −0.79; p = 0.035). In contrast, the context-mean effect was uncorrelated with dopamine release capacity (ρ = −0.32; p = 0.21). These results thus suggest that increased dopamine tone in the striatum may disrupt phasic encoding of contextual uncertainty specifically such that high dopamine releasers systematically overestimate precision of predictions, thus failing to dampen perceptual biases toward expected sensory states under higher uncertainty (i.e., they show reduced uncertainty adjustment consistent with the hypothesized model; Figure 1D). General accuracy measures were unrelated to PET measures (all $\rho < |0.32|$). Amphetamine-induced changes in uncertainty adjustment did not correlate with dopamine release capacity (ρ = 0.24; p = 0.33). Altogether, these data suggest that individuals with higher striatal dopamine function (indicated by dopamine release capacity but also D2-receptor density; see Table S1) have more severe hallucinations (in the case of patients) and a more pronounced reduction in uncertainty adjustment.

Relationship to Gray Matter Volume

To identify structural brain correlates of the uncertainty adjustment, we performed a voxel-based morphometry (VBM) analysis on anatomical images collected for all subjects in study 2. Smaller gray matter volume in the medial prefrontal cortex bilaterally, encompassing the dorsal anterior cingulate cortex (dACC) and extending into the supplementary motor area, correlated with reduced uncertainty adjustment, even after controlling for group and the context-mean effect (analysis of covariance [ANCOVA]; cluster-level p_{FWE} = 0.041; Figure 5). Taking the average gray matter volume within this cluster for each subject, a post hoc analysis found that this volume remained correlated to the uncertainty adjustment in the subgroup of healthy controls

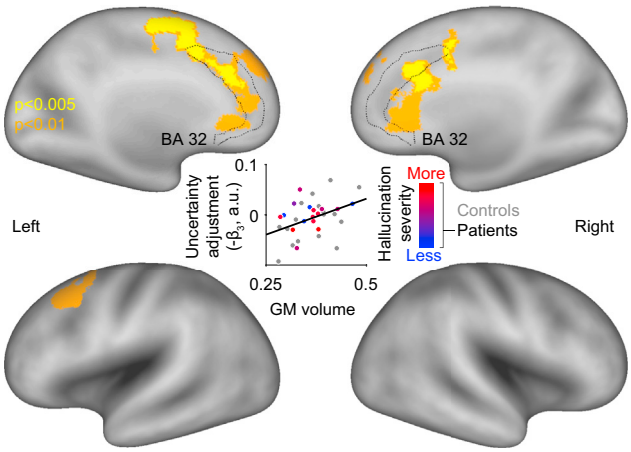

Figure 5. Structural Brain Correlates of the Uncertainty Adjustment
A significant cluster (p_{FWE} = 0.041; peak voxel MNI coordinates [*x*,*y*,*z*]: −9, −17, 62 mm; t_{27} = 4.85; z = 4.08) where reduced gray matter volume is associated with reduced uncertainty adjustment across all subjects is rendered in yellow on a standard cortical surface map (PALS-B12 atlas; rendering performed using Caret software, version 5.65). This significant cluster was obtained using a cluster-forming (height) threshold of $p \leq 0.005$ and extent threshold of 5 adjacent voxels. For illustrative purposes, a significant cluster obtained using a cluster-forming threshold of $p \leq 0.01$ is also shown in orange. For reference, the dotted line delineates Brodmann area (BA) 32, which encompasses the dACC. The central scatterplot shows the correlation between the average gray matter volume within the yellow cluster and uncertainty adjustment across subjects (r = 0.41; p = 0.019; note that these statistics are only shown for completeness as the *a priori* test is the voxelwise analysis).

alone (partial correlation, r = 0.67; p = 0.008), suggesting this relationship was not driven by pathological features of the illness. Gray matter in this cluster was still related to uncertainty adjustment across patients and controls when contrasters were excluded (partial correlation; r = 0.63; p = 0.0004; n = 30). Finally, gray matter volume in this cluster also remained correlated to uncertainty adjustment when controlling for dopamine release capacity (r = 0.53; p = 0.028; partial correlation; patients and controls combined), ruling out dopamine release capacity as a confound in this relationship. No clusters showed a significant negative correlation with uncertainty adjustment, any correlations with the context-mean effect, or group differences.

DISCUSSION

Building on prior work in at-risk populations [25], here, we found that the severity of hallucinations in schizophrenia specifically correlated with a stronger perceptual bias toward expected states (greater assimilation bias) and with failures to dampen this perceptual bias in uncertain contexts (reduced uncertainty adjustment). These findings support the idea that hallucinations may represent percepts under excessive influence of top-down prior expectations [22, 24, 25] and that this influence may be more pronounced in uncertain contexts that should normally reduce the influence of expectations on perception, in agreement with a Bayesian model of hallucinations [17]. Indeed, it was in uncertain contexts where the assimilation bias was strongest in hallucinating patients compared to non-hallucinating patients and healthy subjects. Furthermore, we showed for the first time that a distinct pattern of perceptual bias associated with hallucinations—a reduced uncertainty adjustment—could be induced by amphetamine and was correlated with dopamine release capacity in the associative striatum, the primary site of dopaminergic dysregulation in schizophrenia [6, 7]. Propensity for this perceptual bias was further associated with reduced gray matter volume in the dACC, a brain region involved in adjusting Bayesian learning according to the level of uncertainty [39–41].

Altogether, these findings are consistent with a role for dopamine in signaling precision and ascribe a computational mechanism to a key neurobiological pathway in psychosis. In particular, our findings suggest that inability to downregulate striatal dopamine tone in psychotic patients may disrupt encoding of contextual uncertainty, likely signaled by context-dependent phasic dopamine transients, the gain of which is thought to depend on tonic dopamine [42]. This disruption would lead to a systematic overestimation of precision of predictions and increased gain on top-down signals, which may cause vulnerable individuals to experience hallucinatory percepts reflecting extreme perceptual biases toward sensory expectations. More generally, they extend prior work [43–46] indicating that dopamine plays a modulatory role in perception beyond its well-established role in reward-based learning and decision making. Future work should further dissect the neural circuitry involved in encoding of contextual uncertainty as it relates to perception. Previous work has shown that the dACC plays a critical role in uncertainty-dependent adjustments in learning [39–41]. Thus, our finding that reduced volume of this region is proportional to reductions in the uncertainty adjustment provides further biological plausibility for our behavioral findings by suggesting that, akin to its role in uncertainty adjustments during learning [39–41], the dACC may also support uncertainty adjustments in perception, perhaps through its interactions with the striatum [47].

Dopamine has been increasingly implicated in signaling confidence, certainty, or precision in reward [45, 46] and perceptual tasks [43, 44]. Converging evidence suggests a role for the dopamine-rich striatum in sensory processing [48–50]. Besides its undisputed involvement in perceptual (and ideational) symptoms of psychosis [6], the striatum is a central part of cortico-striato-thalamo-cortical loops interfacing between sensory inputs and their cortical targets [8, 49]. Moreover, dopamine [29] and the striatum play a key role in perception of temporal precision [27, 28] and regularity [50, 51] and may thereby facilitate auditory discrimination [48]. However, the influence of dopamine on hallucinations may not apply universally because dopamine levels in healthy individuals did not relate to hallucination-like experiences [52], underscoring a possible role of illness-specific vulnerability factors or perhaps differences between such phenomena and clinical hallucinations [53].

The coexistence of assimilation and contrast biases in our sample may not be immediately reconciled within a standard Bayesian framework [15, 35], although these effects both represent known forms of contextual influence on perception [54]. Whereas interindividual variability in sensitivity [33, 55, 56] can explain differences between assimilators [30–32] and contrasters [34] in other paradigms, we failed to find a correlation with

duration sensitivity in ours. Thus, an explanation in terms of two separate underlying mechanisms [15] or one where assimilators and contrasters have different balance of bottom-up prediction-error signals versus top-down predictions seem more tenable. A recently extended Bayesian model proposes that many factors may contribute to contrast bias, including increased (internal) sensory noise or differently shaped prior or likelihood functions [35]. The presence of contrast bias dissuaded us from fitting the model to our data because formally capturing these effects would require extending the model with additional features. Contrast biases, however, do not greatly complicate interpretation of our findings with respect to dopamine function in schizophrenia, because they were controlled for in the analyses of uncertainty adjustment, no patients showed significant contrast bias, and all of our findings remained significant after excluding contrasters. Moreover, the presence of contrast bias in some healthy participants may indeed help clarify the role of dopamine in uncertainty adjustments: signed, but not unsigned, uncertainty adjustments relate to dopamine release capacity, implicating a directional effect of dopamine such that excess dopamine may interfere with dampening of assimilation biases specifically rather than with dampening of any biases (assimilation or contrast) irrespective of their direction.

Contrary to some studies suggesting immunity to illusions in schizophrenia [57–59], yet consistent with others [25, 60–62], we found that hallucinations correlated with *increased* susceptibility to (assimilation) illusions. Mixed findings could indicate that distinct neurobiological mechanisms underlie different types of illusions [20, 24]. The evidence for immunity to illusions in schizophrenia, which has been taken to support enhanced bottom-up signaling [26], has been largely derived from low-level visual illusions [57–59] that may depend on local processes within low-level visual regions rather than on top-down modulations [25, 58]. In contrast, context-dependent, top-down modulation may be evoked by tasks that manipulate contextual information sequentially [25], like ours. These types of top-down modulations are instead typically *increased* in individuals with psychosis [25, 60, 61, 63] (but see [64, 65]), correlate with psychosis severity [25, 60, 66], and precede psychosis onset [25, 61, 63]. Conversely, less evidence supports a relationship between immunity to low-level illusions and psychosis severity [67]. One possibility to reconcile these findings [25] is that increased top-down effects in psychosis may be compounded by early deficits in low-level sensory processing, leading to decreased sensory gain [57–59].

Previous work has begun to delineate molecular mechanisms of auditory predictive coding. The mismatch negativity (MMN) event-related potential component from the oddball paradigm may reflect a learning signal (akin to a prediction error) [68–70] that can be disrupted via glutamate NMDA-receptor blockade [71, 72]. Robust evidence points to a MMN deficit in schizophrenia [73, 74], but the magnitude of this deficit has not been consistently related to hallucinations [74] or dopamine [13]. This may be due to failure of standard oddball paradigms to manipulate contextual uncertainty, a central aspect of Bayesian inference in psychosis models [12, 17, 18]. In line with previous data [43–46], fluctuations in dopamine levels could thus signal the precision of predictive information by adjusting the gain on signals according to their reliability, for instance by amplifying top-down signals in highly stable contexts [18, 25], similar to modulations seen in the reward system [45, 46]. If indeed sustained high-dopamine tone in schizophrenia impedes contextual-uncertainty-dependent modulations of dopamine transients, this could lead to overestimation of precision and abnormally strong top-down signals (the opposite effects have been observed with D2-receptor blockade [27]). This scenario—in addition to one consisting of abnormal NMDA-related learning signals—could thus impair learning from new sensory evidence, as observed in hallucinating patients [21].

Limitations and Future Directions

The observed association between uncertainty adjustment and hallucinations, but not with a diagnosis of schizophrenia, could be due to our modest sample size; further work is needed to reach definitive conclusions as to whether patients with schizophrenia as a group differ from controls on this measure. If indeed they do not, this could suggest that diagnosis is a moderating factor in this relationship: perhaps reduced uncertainty adjustment could be relatively innocuous in healthy individuals due to an unknown resilience factor lacking in patients, although this possibility remains unclear given the trend-level relationship between hallucination-like experiences and perceptual biases in health (Results; study 1). Alternatively, this pattern of findings could suggest compensatory mechanisms within the patient group (e.g., some patients could develop a supranormal ability for uncertainty adjustments that confers resilience against hallucinations). Finally, some models of schizophrenia propose that opposing patterns of perceptual bias may characterize this illness: weak top-down biases could explain certain trait-like characteristics of schizophrenia, whereas compensatory adaptations leading to excessively strong top-down biases could explain state-dependent (psychotic) experiences such as hallucinations [18]. This pattern, which would obscure group differences between patients as a whole and controls, is consistent with the pattern we observe wherein healthy controls show a perceptual bias under high uncertainty that is greater than that in non-hallucinating patients but smaller than that in hallucinating patients (Figure S1C) and with patterns observed in prior work [22]. Nonetheless, these scenarios—which may not be uncommon in studying mechanisms of specific symptom domains, beyond diagnostic categories—do not preclude conclusions regarding the strong and specific relationship of hallucinations and precision coding we hypothesized *a priori* and empirically observed. There is a major difference in the timescale of the imaging measures we employ compared to the rapid dynamics of context-dependent changes in perception that we study with the VCTR task. Nevertheless, increases in dopamine tone reflected in our PET imaging measure would likely disrupt the phasic dopamine signals that may encode contextual uncertainty [42]. Thus, our multimodal imaging approach is appropriate to investigate the relationship between dopamine dysfunction and failures in uncertainty-dependent adjustments in perception. The experience of hallucinations themselves may have interfered with subjective perception in patients; however, this is unlikely as only two patients reported hallucinations that were frequent enough to interfere with the task. Development of tasks similar to the VCTR but using *verbal* auditory stimuli would be an important direction given the phenomenology and content of auditory

hallucinations in schizophrenia, an element that our task was not designed to investigate. Finally, dopamine release in our study was related to the pre-amphetamine uncertainty adjustment, not the amphetamine-induced change in uncertainty adjustment. This may not be surprising given the indication that the uncertainty adjustment may be susceptible to floor effects (Figure 4A; similar to dopamine's influence on other cognitive processes) [36–38], which may well decrease sensitivity to detect changes in this measure.

In summary, our results provide novel empirical support for a formal account of hallucinations implicating dopamine dysfunctions in signaling of precision of predictions. These results also provide insight into the role of dopamine in perception more generally by suggesting that striatal dopamine may adjust the gain on top-down prediction signals as a function of environmental uncertainty. Altogether, our findings suggest that the well-known excess in striatal dopamine in schizophrenia may disrupt a context-dependent integration of expectations into perceptual experiences, ultimately leading to hallucinatory percepts.

STAR★METHODS

Detailed methods are provided in the online version of this paper and include the following:

- KEY RESOURCES TABLE
- CONTACT FOR REAGENT AND RESOURCE SHARING
- EXPERIMENTAL MODEL AND SUBJECT DETAILS
  - Subjects
- METHOD DETAILS
  - Clinical and cognitive measures
  - Task design
  - Assessment of explicit knowledge of VCTR illusion effect
  - Positron Emission Tomography (PET) imaging
  - Structural Magnetic Resonance Imaging (MRI)
- QUANTIFICATION AND STATISTICAL ANALYSIS
  - Statistical Analysis
  - PET imaging analysis
  - MRI analysis
  - Model description and simulations

SUPPLEMENTAL INFORMATION

Supplemental Information includes one figure and one table and can be found with this article online at https://doi.org/10.1016/j.cub.2017.12.059.

ACKNOWLEDGMENTS

Funding for this study was provided by grants K23-MH101637 (PI: G.H.), P50-MH086404 (PI: A.A.-D.), R21-MH099509 (PI: A.A.-D.), and R01MH068073 (PI: P.D.B.) from the National Institute of Mental Health. C.M.C. was supported by a post-doctoral fellowship from the Fonds de Recherche du Québec, Santé. G.H. was additionally supported by a grant from the Sidney R. Baer Jr. Foundation.

AUTHOR CONTRIBUTIONS

Conceptualization, G.H., C.M.C., and P.D.B.; Methodology, G.H., C.M.C., N.D.D., and P.D.B.; Formal Analysis, G.H., C.M.C., N.D.D., and M.S.; Investigation, G.H., C.M.C., J.J.W., and R.J.R.; Writing – Original Draft, G.H. and C.M.C.; Writing – Review & Editing, G.H., C.M.C., P.D.B., A.A.-D., M.S., N.D.D., J.J.W., and R.J.R.; Funding Acquisition, G.H. and A.A.-D.

DECLARATION OF INTERESTS

The authors declare no competing interests.

Received: August 15, 2017
Revised: November 23, 2017
Accepted: December 29, 2017
Published: February 1, 2018

REFERENCES

1. Picard, F., and Friston, K. (2014). Predictions, perception, and a sense of self. Neurology *83*, 1112–1118.
2. Rothberg, M.B., Arora, A., Hermann, J., Kleppel, R., St Marie, P., and Visintainer, P. (2010). Phantom vibration syndrome among medical staff: a cross sectional survey. BMJ *341*, c6914.
3. Sommer, I.E., Slotema, C.W., Daskalakis, Z.J., Derks, E.M., Blom, J.D., and van der Gaag, M. (2012). The treatment of hallucinations in schizophrenia spectrum disorders. Schizophr. Bull. *38*, 704–714.
4. McKetin, R., Lubman, D.I., Baker, A.L., Dawe, S., and Ali, R.L. (2013). Dose-related psychotic symptoms in chronic methamphetamine users: evidence from a prospective longitudinal study. JAMA Psychiatry *70*, 319–324.
5. Stowe, R.L., Ives, N.J., Clarke, C., van Hilten, J., Ferreira, J., Hawker, R.J., Shah, L., Wheatley, K., and Gray, R. (2008). Dopamine agonist therapy in early Parkinson's disease. Cochrane Database Syst. Rev. (2), CD006564.
6. Kegeles, L.S., Abi-Dargham, A., Frankle, W.G., Gil, R., Cooper, T.B., Slifstein, M., Hwang, D.R., Huang, Y., Haber, S.N., and Laruelle, M. (2010). Increased synaptic dopamine function in associative regions of the striatum in schizophrenia. Arch. Gen. Psychiatry *67*, 231–239.
7. Weinstein, J.J., Chohan, M.O., Slifstein, M., Kegeles, L.S., Moore, H., and Abi-Dargham, A. (2017). Pathway-specific dopamine abnormalities in schizophrenia. Biol. Psychiatry *81*, 31–42.
8. Maia, T.V., and Frank, M.J. (2017). An integrative perspective on the role of dopamine in schizophrenia. Biol. Psychiatry *81*, 52–66.
9. Schultz, W. (2013). Updating dopamine reward signals. Curr. Opin. Neurobiol. *23*, 229–238.
10. Hamid, A.A., Pettibone, J.R., Mabrouk, O.S., Hetrick, V.L., Schmidt, R., Vander Weele, C.M., Kennedy, R.T., Aragona, B.J., and Berke, J.D. (2016). Mesolimbic dopamine signals the value of work. Nat. Neurosci. *19*, 117–126.
11. Daw, N.D., and Doya, K. (2006). The computational neurobiology of learning and reward. Curr. Opin. Neurobiol. *16*, 199–204.
12. Friston, K.J., Shiner, T., FitzGerald, T., Galea, J.M., Adams, R., Brown, H., Dolan, R.J., Moran, R., Stephan, K.E., and Bestmann, S. (2012). Dopamine, affordance and active inference. PLoS Comput. Biol. *8*, e1002327.
13. Kenemans, J.L., and Kähkönen, S. (2011). How human electrophysiology informs psychopharmacology: from bottom-up driven processing to top-down control. Neuropsychopharmacology *36*, 26–51.
14. Sharpe, M.J., Chang, C.Y., Liu, M.A., Batchelor, H.M., Mueller, L.E., Jones, J.L., Niv, Y., and Schoenbaum, G. (2017). Dopamine transients are sufficient and necessary for acquisition of model-based associations. Nat. Neurosci. *20*, 735–742.
15. Stocker, A.A., and Simoncelli, E.P. (2006). Sensory adaptation within a Bayesian framework for perception. In Advances in Neural Information Processing Systems, Y. Weiss, B. Schölkopf, and J. Platt, eds. (MIT Press), pp. 1291–1298.
16. Zelano, C., Mohanty, A., and Gottfried, J.A. (2011). Olfactory predictive codes and stimulus templates in piriform cortex. Neuron *72*, 178–187.

17. Friston, K.J. (2005). Hallucinations and perceptual inference. Behav. Brain Sci. *28*, 764–766.
18. Adams, R.A., Stephan, K.E., Brown, H.R., Frith, C.D., and Friston, K.J. (2013). The computational anatomy of psychosis. Front. Psychiatry *4*, 47.
19. Fletcher, P.C., and Frith, C.D. (2009). Perceiving is believing: a Bayesian approach to explaining the positive symptoms of schizophrenia. Nat. Rev. Neurosci. *10*, 48–58.
20. Teufel, C., and Nanay, B. (2017). How to (and how not to) think about top-down influences on visual perception. Conscious. Cogn. *47*, 17–25.
21. Horga, G., Schatz, K.C., Abi-Dargham, A., and Peterson, B.S. (2014). Deficits in predictive coding underlie hallucinations in schizophrenia. J. Neurosci. *34*, 8072–8082.
22. Powers, A.R., Mathys, C., and Corlett, P.R. (2017). Pavlovian conditioning-induced hallucinations result from overweighting of perceptual priors. Science *357*, 596–600.
23. Corlett, P.R., Frith, C.D., and Fletcher, P.C. (2009). From drugs to deprivation: a Bayesian framework for understanding models of psychosis. Psychopharmacology (Berl.) *206*, 515–530.
24. Powers, A.R., III, Kelley, M., and Corlett, P.R. (2016). Hallucinations as top-down effects on perception. Biol. Psychiatry Cogn. Neurosci. Neuroimaging *1*, 393–400.
25. Teufel, C., Subramaniam, N., Dobler, V., Perez, J., Finnemann, J., Mehta, P.R., Goodyer, I.M., and Fletcher, P.C. (2015). Shift toward prior knowledge confers a perceptual advantage in early psychosis and psychosis-prone healthy individuals. Proc. Natl. Acad. Sci. USA *112*, 13401–13406.
26. Jardri, R., and Denève, S. (2013). Circular inferences in schizophrenia. Brain *136*, 3227–3241.
27. Tomassini, A., Ruge, D., Galea, J.M., Penny, W., and Bestmann, S. (2016). The role of dopamine in temporal uncertainty. J. Cogn. Neurosci. *28*, 96–110.
28. Tomasi, D., Wang, G.J., Studentsova, Y., and Volkow, N.D. (2015). Dissecting neural responses to temporal prediction, attention, and memory: effects of reward learning and interoception on time perception. Cereb. Cortex *25*, 3856–3867.
29. Coull, J.T., Cheng, R.K., and Meck, W.H. (2011). Neuroanatomical and neurochemical substrates of timing. Neuropsychopharmacology *36*, 3–25.
30. Acerbi, L., Wolpert, D.M., and Vijayakumar, S. (2012). Internal representations of temporal statistics and feedback calibrate motor-sensory interval timing. PLoS Comput. Biol. *8*, e1002771.
31. Akdoğan, B., and Balcı, F. (2016). Stimulus probability effects on temporal bisection performance of mice (Mus musculus). Anim. Cogn. *19*, 15–30.
32. Lejeune, H., and Wearden, J.H. (2009). Vierordt's *The Experimental Study of the Time Sense* (1868) and its legacy. Eur. J. Cogn. Psychol. *21*, 941–960.
33. Schab, F.R., and Crowder, R.G. (1988). The role of succession in temporal cognition: is the time-order error a recency effect of memory? Percept. Psychophys. *44*, 233–242.
34. Nakajima, Y., Hasuo, E., Yamashita, M., and Haraguchi, Y. (2014). Overestimation of the second time interval replaces time-shrinking when the difference between two adjacent time intervals increases. Front. Hum. Neurosci. *8*, 281.
35. Wei, X.X., and Stocker, A.A. (2015). A Bayesian observer model constrained by efficient coding can explain 'anti-Bayesian' percepts. Nat. Neurosci. *18*, 1509–1517.
36. Cools, R., and D'Esposito, M. (2011). Inverted-U-shaped dopamine actions on human working memory and cognitive control. Biol. Psychiatry *69*, e113–e125.
37. Rolls, E.T., Loh, M., Deco, G., and Winterer, G. (2008). Computational models of schizophrenia and dopamine modulation in the prefrontal cortex. Nat. Rev. Neurosci. *9*, 696–709.
38. Sawaguchi, T., and Goldman-Rakic, P.S. (1991). D1 dopamine receptors in prefrontal cortex: involvement in working memory. Science *251*, 947–950.
39. Behrens, T.E., Woolrich, M.W., Walton, M.E., and Rushworth, M.F. (2007). Learning the value of information in an uncertain world. Nat. Neurosci. *10*, 1214–1221.
40. Kolling, N., Wittmann, M.K., Behrens, T.E., Boorman, E.D., Mars, R.B., and Rushworth, M.F. (2016). Value, search, persistence and model updating in anterior cingulate cortex. Nat. Neurosci. *19*, 1280–1285.
41. Ebitz, R.B., and Hayden, B.Y. (2016). Dorsal anterior cingulate: a Rorschach test for cognitive neuroscience. Nat. Neurosci. *19*, 1278–1279.
42. Grace, A.A. (2016). Dysregulation of the dopamine system in the pathophysiology of schizophrenia and depression. Nat. Rev. Neurosci. *17*, 524–532.
43. Andreou, C., Bozikas, V.P., Luedtke, T., and Moritz, S. (2015). Associations between visual perception accuracy and confidence in a dopaminergic manipulation study. Front. Psychol. *6*, 414.
44. Lou, H.C., Skewes, J.C., Thomsen, K.R., Overgaard, M., Lau, H.C., Mouridsen, K., and Roepstorff, A. (2011). Dopaminergic stimulation enhances confidence and accuracy in seeing rapidly presented words. J. Vis. *11*, 15.
45. Diederen, K.M., Spencer, T., Vestergaard, M.D., Fletcher, P.C., and Schultz, W. (2016). Adaptive prediction error coding in the human midbrain and striatum facilitates behavioral adaptation and learning efficiency. Neuron *90*, 1127–1138.
46. Fiorillo, C.D., Tobler, P.N., and Schultz, W. (2003). Discrete coding of reward probability and uncertainty by dopamine neurons. Science *299*, 1898–1902.
47. Kunishio, K., and Haber, S.N. (1994). Primate cingulostriatal projection: limbic striatal versus sensorimotor striatal input. J. Comp. Neurol. *350*, 337–356.
48. Geiser, E., Notter, M., and Gabrieli, J.D. (2012). A corticostriatal neural system enhances auditory perception through temporal context processing. J. Neurosci. *32*, 6177–6182.
49. Lim, S.J., Fiez, J.A., and Holt, L.L. (2014). How may the basal ganglia contribute to auditory categorization and speech perception? Front. Neurosci. *8*, 230.
50. Sameiro-Barbosa, C.M., and Geiser, E. (2016). Sensory entrainment mechanisms in auditory perception: neural synchronization cortico-striatal activation. Front. Neurosci. *10*, 361.
51. Meck, W.H., Penney, T.B., and Pouthas, V. (2008). Cortico-striatal representation of time in animals and humans. Curr. Opin. Neurobiol. *18*, 145–152.
52. Howes, O.D., Shotbolt, P., Bloomfield, M., Daalman, K., Demjaha, A., Diederen, K.M., Ibrahim, K., Kim, E., McGuire, P., Kahn, R.S., and Sommer, I.E. (2013). Dopaminergic function in the psychosis spectrum: an [18F]-DOPA imaging study in healthy individuals with auditory hallucinations. Schizophr. Bull. *39*, 807–814.
53. David, A.S. (2010). Why we need more debate on whether psychotic symptoms lie on a continuum with normality. Psychol. Med. *40*, 1935–1942.
54. Helson, H. (1964). Current trends and issues in adaptation-level theory. Am. Psychol. *19*, 26–38.
55. Howe, C.Q., and Purves, D. (2004). Size contrast and assimilation explained by the statistics of natural scene geometry. J. Cogn. Neurosci. *16*, 90–102.
56. Jaeger, T.B. (1999). Assimilation and contrast in geometrical illusions: a theoretical analysis. Percept. Mot. Skills *89*, 249–261.
57. Dakin, S., Carlin, P., and Hemsley, D. (2005). Weak suppression of visual context in chronic schizophrenia. Curr. Biol. *15*, R822–R824.
58. Kantrowitz, J.T., Butler, P.D., Schecter, I., Silipo, G., and Javitt, D.C. (2009). Seeing the world dimly: the impact of early visual deficits on visual experience in schizophrenia. Schizophr. Bull. *35*, 1085–1094.
59. Keane, B.P., Silverstein, S.M., Wang, Y., and Papathomas, T.V. (2013). Reduced depth inversion illusions in schizophrenia are state-specific and occur for multiple object types and viewing conditions. J. Abnorm. Psychol. *122*, 506–512.

60. Fonseca-Pedrero, E., Badoud, D., Antico, L., Caputo, G.B., Eliez, S., Schwartz, S., and Debbané, M. (2015). Strange-face-in-the-mirror illusion and schizotypy during adolescence. Schizophr. Bull. *41* (*Suppl 2*), S475–S482.
61. Hoffman, R.E., Woods, S.W., Hawkins, K.A., Pittman, B., Tohen, M., Preda, A., Breier, A., Glist, J., Addington, J., Perkins, D.O., and McGlashan, T.H. (2007). Extracting spurious messages from noise and risk of schizophrenia-spectrum disorders in a prodromal population. Br. J. Psychiatry *191*, 355–356.
62. Vercammen, A., and Aleman, A. (2010). Semantic expectations can induce false perceptions in hallucination-prone individuals. Schizophr. Bull. *36*, 151–156.
63. Parnas, J., Vianin, P., Saebye, D., Jansson, L., Volmer-Larsen, A., and Bovet, P. (2001). Visual binding abilities in the initial and advanced stages of schizophrenia. Acta Psychiatr. Scand. *103*, 171–180.
64. Dima, D., Dietrich, D.E., Dillo, W., and Emrich, H.M. (2010). Impaired top-down processes in schizophrenia: a DCM study of ERPs. Neuroimage *52*, 824–832.
65. Sanders, L.L., de Millas, W., Heinz, A., Kathmann, N., and Sterzer, P. (2013). Apparent motion perception in patients with paranoid schizophrenia. Eur. Arch. Psychiatry Clin. Neurosci. *263*, 233–239.
66. Norton, D., Ongur, D., Stromeyer, C., 3rd, and Chen, Y. (2008). Altered 'three-flash' illusion in response to two light pulses in schizophrenia. Schizophr. Res. *103*, 275–282.
67. Notredame, C.E., Pins, D., Deneve, S., and Jardri, R. (2014). What visual illusions teach us about schizophrenia. Front. Integr. Nuerosci. *8*, 63.
68. Haenschel, C., Vernon, D.J., Dwivedi, P., Gruzelier, J.H., and Baldeweg, T. (2005). Event-related brain potential correlates of human auditory sensory memory-trace formation. J. Neurosci. *25*, 10494–10501.
69. Imada, T., Hari, R., Loveless, N., McEvoy, L., and Sams, M. (1993). Determinants of the auditory mismatch response. Electroencephalogr. Clin. Neurophysiol. *87*, 144–153.
70. Schmidt, A., Bachmann, R., Kometer, M., Csomor, P.A., Stephan, K.E., Seifritz, E., and Vollenweider, F.X. (2012). Mismatch negativity encoding of prediction errors predicts S-ketamine-induced cognitive impairments. Neuropsychopharmacology *37*, 865–875.
71. Javitt, D.C., Steinschneider, M., Schroeder, C.E., and Arezzo, J.C. (1996). Role of cortical N-methyl-D-aspartate receptors in auditory sensory memory and mismatch negativity generation: implications for schizophrenia. Proc. Natl. Acad. Sci. USA *93*, 11962–11967.
72. Rosburg, T., and Kreitschmann-Andermahr, I. (2016). The effects of ketamine on the mismatch negativity (MMN) in humans - A meta-analysis. Clin. Neurophysiol. *127*, 1387–1394.
73. Erickson, M.A., Ruffle, A., and Gold, J.M. (2016). A meta-analysis of mismatch negativity in schizophrenia: from clinical risk to disease specificity and progression. Biol. Psychiatry *79*, 980–987.
74. Umbricht, D., and Krljes, S. (2005). Mismatch negativity in schizophrenia: a meta-analysis. Schizophr. Res. *76*, 1–23.
75. First, M., Spitzer, R., Gibbon, M., and Williams, J. (1995). Structured Clinical Interview for DSM-IV Axis I Disorders (SCID-I/P, Version 2.0) (Biometrics Research Dept., New York State Psychiatric Institute).
76. Nurnberger, J.I., Jr., Blehar, M.C., Kaufmann, C.A., York-Cooler, C., Simpson, S.G., Harkavy-Friedman, J., Severe, J.B., Malaspina, D., and Reich, T. (1994). Diagnostic interview for genetic studies. Rationale, unique features, and training. NIMH genetics initiative. Arch. Gen. Psychiatry *51*, 849–859.
77. Wechsler, D. (1999). Wechsler Abbreviated Scale of Intelligence (WASI) (Psychological Corporation).
78. Cohen, J.D., Forman, S.D., Braver, T.S., Casey, B.J., Servan-Schreiber, D., and Noll, D.C. (1994). Activation of the prefrontal cortex in a nonspatial working memory task with functional MRI. Hum. Brain Mapp. *1*, 293–304.
79. Launay, G., and Slade, P. (1981). The measurement of hallucinatory predisposition in male and female prisoners. Pers. Individ. Dif. *2*, 221–234.
80. Kay, S.R., Fiszbein, A., and Opler, L.A. (1987). The positive and negative syndrome scale (PANSS) for schizophrenia. Schizophr. Bull. *13*, 261–276.
81. Nuechterlein, K.H., Green, M.F., Kern, R.S., Baade, L.E., Barch, D.M., Cohen, J.D., Essock, S., Fenton, W.S., Frese, F.J., 3rd, Gold, J.M., et al. (2008). The MATRICS Consensus Cognitive Battery, part 1: test selection, reliability, and validity. Am. J. Psychiatry *165*, 203–213.
82. Hollingshead, A.B. (1975). Four Factor Index of Social Status (Yale University).
83. Jazayeri, M., and Shadlen, M.N. (2010). Temporal context calibrates interval timing. Nat. Neurosci. *13*, 1020–1026.
84. Grondin, S., Ouellet, B., and Roussel, M.-È. (2001). About optimal timing and stability of Weber fraction for duration discrimination. Acoust. Sci. Technol. *22*, 370–372.
85. Cicchini, G.M., Arrighi, R., Cecchetti, L., Giusti, M., and Burr, D.C. (2012). Optimal encoding of interval timing in expert percussionists. J. Neurosci. *32*, 1056–1060.
86. Weinstein, J.J., van de Giessen, E., Rosengard, R.J., Xu, X., Ojeil, N., Brucato, G., Gil, R.B., Kegeles, L.S., Laruelle, M., Slifstein, M., et al. (2017). PET imaging of dopamine-D2 receptor internalization in schizophrenia. Mol. Psychiatry. Published online May 16, 2017. https://doi.org/10.1038/mp.2017.107.
87. Sandiego, C.M., Gallezot, J.D., Lim, K., Ropchan, J., Lin, S.F., Gao, H., Morris, E.D., and Cosgrove, K.P. (2015). Reference region modeling approaches for amphetamine challenge studies with [11C]FLB 457 and PET. J. Cereb. Blood Flow Metab. *35*, 623–629.
88. Martinez, D., Slifstein, M., Broft, A., Mawlawi, O., Hwang, D.R., Huang, Y., Cooper, T., Kegeles, L., Zarahn, E., Abi-Dargham, A., et al. (2003). Imaging human mesolimbic dopamine transmission with positron emission tomography. Part II: amphetamine-induced dopamine release in the functional subdivisions of the striatum. J. Cereb. Blood Flow Metab. *23*, 285–300.
89. Lammertsma, A.A., and Hume, S.P. (1996). Simplified reference tissue model for PET receptor studies. Neuroimage *4*, 153–158.
90. Mawlawi, O., Martinez, D., Slifstein, M., Broft, A., Chatterjee, R., Hwang, D.R., Huang, Y., Simpson, N., Ngo, K., Van Heertum, R., and Laruelle, M. (2001). Imaging human mesolimbic dopamine transmission with positron emission tomography: I. Accuracy and precision of D(2) receptor parameter measurements in ventral striatum. J. Cereb. Blood Flow Metab. *21*, 1034–1057.
91. Ashburner, J., and Friston, K.J. (2000). Voxel-based morphometry–the methods. Neuroimage *11*, 805–821.
92. Ashburner, J. (2007). A fast diffeomorphic image registration algorithm. Neuroimage *38*, 95–113.
93. Karaminis, T., Cicchini, G.M., Neil, L., Cappagli, G., Aagten-Murphy, D., Burr, D., and Pellicano, E. (2016). Central tendency effects in time interval reproduction in autism. Sci. Rep. *6*, 28570.
94. Dayan, P., and Abbott, L.F. (2001). Theoretical Neuroscience: Computational and Mathematical Modeling of Neural Systems (Massachusetts Institute of Technology Press).

STAR★METHODS

KEY RESOURCES TABLE

REAGENT or RESOURCE	SOURCE	IDENTIFIER
Software and Algorithms		
MATLAB	MathWorks	https://www.mathworks.com/products/matlab.html
SPM12	the Wellcome Trust Centre for Neuroimaging	http://www.fil.ion.ucl.ac.uk/spm/software/
SPM2	the Wellcome Trust Centre for Neuroimaging	http://www.fil.ion.ucl.ac.uk/spm/software/
E-prime 1	Psychology Software Tools	https://pstnet.com/products/e-prime/

CONTACT FOR REAGENT AND RESOURCE SHARING

Further information and requests for resources and reagents should be directed to and will be fulfilled by the Lead Contact, Guillermo Horga (horgag@nyspi.columbia.edu).

EXPERIMENTAL MODEL AND SUBJECT DETAILS

Subjects

This study was approved by the Institutional Review Board of the New York State Psychiatric Institute (NYSPI) at Columbia University Medical Center (CUMC). All participants provided written informed consent. See Table 1 for demographic and clinical information. The inclusion criteria for patients with schizophrenia were: age 18-55 years; DSM-IV criteria for schizophrenia, schizophreniform or schizoaffective disorder; negative urine toxicology, stable, outpatient medication-free status for at least three weeks. Patients with schizophrenia were excluded for a diagnosis of bipolar disorder, active substance use disorders (except tobacco use disorders) or current use based on urine toxicology. Healthy controls were excluded for: current or past axis I disorder (except tobacco use disorder), as verified using the Structured Clinical Interview for DSM-IV Disorders (SCID-IV) [75, 76], history of neurological disorders or current major medical illness, and first degree relatives with a history of psychotic disorder. Patients were recruited from the outpatient research facilities at NYSPI; healthy controls were recruited through advertisements and word of mouth. Healthy volunteers in Studies 1 and 2 comprised two separate groups with the exception of two subjects whose data was used in both studies.

METHOD DETAILS

Clinical and cognitive measures

In Study 1 cognitive performance was assessed with the Wechsler abbreviated scale of intelligence (WASI-II) [77] and the n-back test of working memory (letter version) [78]. Subclinical hallucination-like experiences were assessed with the Launay-Slade Hallucinations Scale (LSHS) [79]. Subjects also reported sleep quality. In Study 2 psychopathology including hallucination severity was measured with the Positive and Negative Syndrome Scale (PANSS) [80]. Cognitive abilities were assessed with the Measurement and Treatment Research to Improve Cognition in Schizophrenia (MATRICS) Consensus Cognitive Battery [81]. Socio-economic status of all participants and their parents was measured with the Hollingshead interview [82].

Task design

We designed an auditory task inspired by the oddball paradigm [73] and by previous interval-reproduction tasks [83] in which subjects were instructed to report their perception of the duration of a pure tone (1000 Hz, 65 dB; see Figures 1A and 1B for task schematic). The duration of the "target" tone to be reproduced was held constant at 700 ms in 90% of trials. In the remaining 10% of trials ("catch" trials), the duration of the target tone varied so as to provide a measure of sensitivity to target tone duration throughout the experiment (*"catch" trial effect*). Following each target tone, subjects listened to a visually cued "response" tone that played until subjects terminated it with a key press when they judged that its duration matched that of the target tone. The interval between the onset of this response tone and its termination by key press defined the reproduction duration. Prior to target tones, subjects listened to a train of 2–4 context tones that they were not asked to remember or respond to. Thus, each trial consisted of a train of context tones, one target tone and one response tone. The target tone was distinguished from context tones by a visual cue (a gray square and the word "listen"). Regardless of tone durations, stimulus onsets were always separated by a constant interval of 1,700 ms. An experimental session consisted of 2 blocks of 60 trials each, which lasted about 17 minutes. E-prime 1 software was used for stimulus presentation.

Our key experimental manipulations were applied to the context-tone trains. These varied in their mean duration (context mean, short: 543 ms, medium: 700 ms, or long: 980 ms), the variability across tones within the train (context variance: low [SD of 0 ms], high

[SD of 86, 111, 156 ms respectively for short, medium, and long context mean]), and the number of tones comprising the train (2, 3, or 4). Fluctuations in context tone duration were scaled according to Weber's law as γ (SD/mean), analogous to the Weber fraction and shown to be constant over this range of auditory stimulus durations [84]. The 29% difference in duration between the short and long context means compared to target tones was intentionally well above previously reported thresholds for duration discrimination (~8%–16% [84]). Note that although longer interval durations are associated with higher estimation uncertainty [83], this appears to apply more to visual than to auditory stimuli [85] similar to those in our task.

Unlike in standard oddball paradigms and following the illusion literature, we systematically manipulated context tones while keeping the target tone constant so as to induce changes in perception driven by the statistics of the prior rather than by those of the observed stimulus. To help ensure subjects were consistently following task instructions, they were informed that although the task was subjective and there were no wrong answers, consistently providing random or extreme responses would result in loss of a $10 bonus (although the bonus was actually given to all participants regardless of their performance). For further details see Figures 1A and 1B.

General accuracy measures

Prior to the VCTR task, subjects performed a brief practice session during which they familiarized themselves with the process of reproducing tones both in the presence and absence of context tones. They also performed a duration-sensitivity task in which individual tones were presented and immediately reproduced in the absence of context tones. This was repeated for 24 tones ranging in duration from 500 ms to 1,500 ms (similar to the range in the VCTR task). Duration sensitivity was calculated by regressing subjects' reproduction durations against true tone durations. Aside from duration sensitivity, other *general accuracy measures* unrelated to our measures of interest (i.e., uncertainty adjustment and context mean effect) included measures derived from the VCTR task itself: the "catch" trial effect (see Task design section of Methods), response variability (root mean squared error in the main regression model), mean reproduction duration, and number of omitted responses.

Motor-control task

A subsample of 10 healthy individuals from Study 1 also completed a control variant of the VCTR (motor-control task) in which the same trains of context tones were presented over 120 trials but instead of reproducing the duration of a target tone following the context tones, subjects simply had to indicate by a key press when a line had extended from the edge to the middle of the screen (which corresponded to a 700-ms interval, except on 10% of trials). This task aimed to determine whether context tones could bias motor responding or magnitude judgments in general, in which case apparent perceptual biases during the VCTR task could have been confounded by motor or more general biases.

Assessment of explicit knowledge of VCTR illusion effect

Following completion of the VCTR task, all subjects answered multiple-choice questions about their subjective experience of the task. Some questions pertained to subjects' awareness of an illusion, for instance whether they noticed that target tones sounded longer, shorter, or the same as usual when they were preceded by long context tones. A self-reported contrast-assimilation score on the VCTR was derived such that subjects who noticed target tones preceded by long context tones sounding longer and target tones preceded by short context tones sounding shorter (noticed an assimilation bias on both long and short context trials) had a maximal score of 2, subjects who consistently perceived target tones durations shifting in the opposite direction from context tones (a contrast bias) had a minimal score of -2, and subjects had a score of 0 if they did not notice contextual effects on auditory perception or had inconsistent effects (indicative of contrast and assimilation).

Positron Emission Tomography (PET) imaging

Eighteen subjects from Study 2 (8 healthy controls, 10 patients) underwent PET scans on a Biograph mCT PET-CT scanner (Siemens/CTI, Knoxville TN) with [^{11}C]raclopride: a baseline (pre-amphetamine) PET scan on one day, and a post-amphetamine PET scan acquired the following day (detailed methods for this experiment are published [86]), 5-7 hours after oral administration of amphetamine (0.5 mg/kg). The VCTR was administered the day prior to amphetamine administration (pre-amphetamine condition) and again 100 minutes following amphetamine administration (post-amphetamine condition). This time point was chosen to fall within or near the peak plasma amphetamine level [87]. Figure 1C illustrates the timing of PET scans and VCTR task sessions. Table 1 shows PET scan parameters.

Structural Magnetic Resonance Imaging (MRI)

We acquired high-resolution anatomical T1-weighted images on a GE Healthcare 3T MR750 scanner using a 32-channel, phased-array Nova head coil. The T1-weighted 3D BRAVO sequence had the following parameters: TI = 450 ms, minimum TR and TE, flip angle = 12°, FoV = 24 cm, matrix = 300 × 300, number of slices = 220, isotropic voxel size = 0.8 mm^3. This sequence uses minimum values for repetition time and echo time, which therefore vary slightly from one scan to the next. The echo time in our scans was 3.09-3.10 s and the repetition time was 7.83-7.86 s.

QUANTIFICATION AND STATISTICAL ANALYSIS

Statistical Analysis

All analyses were carried out using MATLAB. To analyze the VCTR-task data, regression analyses predicting the subject's reproduction duration across all trials (except for those with omitted responses and 'catch' trials) were performed separately for each subject using robust multiple linear regression based on iteratively reweighted least-squares with a bisquare-weighting function. The independent variables in the main model were context mean (short, medium, long), context variance (low, high), and the interaction of context mean by context variance: $\textit{Reproduction duration} \sim \beta_1 \cdot \textit{context mean} + \beta_2 \cdot \textit{context variance} + \beta_3 \cdot \textit{context mean} \cdot \textit{context variance}$. The number of tones in context tone trains (context length) did not influence reproduction durations and was therefore omitted from the model.

To determine whether the illusion effects observed –which we found went both in the direction of assimilation and of contrast– were more extreme than would be expected by chance, we used a permutation analysis to identify the distribution of context mean β_1 values that would be expected by chance, running the main regression model on 10,000 surrogate subjects for which the labels of context conditions (both for context-mean and context-variance) were randomly shuffled across trials. Levene's test was then used to compare the variance in real and permuted data.

The unstandardized regression coefficients (β) for the context-mean variable (β_1) and the context-mean × context-variance interaction ($-\beta_3$, referred to henceforth as *uncertainty adjustment*, our main variable of interest, which we made negative so that uncertainty-related changes in the expected direction in assimilators had a positive value) were estimated for each subject and submitted to group-level analysis. Note that β_1 (i.e., the *context-mean effect*) represents the influence of context-mean in the low-variance condition, where perceptual biases are typically stronger. A positive context-mean effect implies the presence of a bias whereby the perceived duration of target tones is biased in the direction of the mean duration of context tones (*assimilation*). In assimilators, a positive uncertainty adjustment is the normative pattern, which reflects dampening of the assimilation bias under high compared to low variance, while a negative uncertainty adjustment would suggest a paradoxical increase in the assimilation bias under high compared to low variance. (In contrasters, on the other hand, a negative uncertainty adjustment would be normative and a positive one would be paradoxical.) Because assimilation is the more prevalent bias in our data (and the only one observed in patients), we take less positive uncertainty adjustments to be less normative and refer to them as *reduced uncertainty adjustment*.

Group-level analyses compared differences in β values by group membership (one-way ANOVA or two-sample t test) or task condition (paired t test), robust linear regression to examine amphetamine-induced change in uncertainty adjustment as a function of pre-amphetamine uncertainty adjustment, and partial correlations to relate task measures to clinical and PET measures. Analyses relating task measures to clinical or PET dopamine measures were non-parametric (Spearman's rank correlations) due to non-normality in PET and clinical measures (based on Lilliefors tests) and the use of the PANSS hallucinations item (P3), an ordinal measure.

PET imaging analysis

List mode data were acquired over 60 min following a single bolus injection of [^{11}C]raclopride, binned into a sequence of frames of increasing duration and reconstructed by filtered back projection using manufacturer-provided software. PET data were motion-corrected and registered to the individuals' T1-weighted MRI scan (see Structural MRI section) using SPM2. Regions of interest (ROIs) were drawn on each subject's T1-weighted MRI scan and transferred to the coregistered PET data. Time activity curves were formed as the mean activity in each ROI in each frame. In line with our hypothesis, our *a priori* ROI was the associative striatum, defined as previously [6, 88], as the entire caudate nucleus and the precommissural putamen. Data were analyzed using the simplified reference tissue model (SRTM) [89, 90] with cerebellum as a reference tissue to determine the binding potential relative to the non-displaceable compartment (BP_{ND}). The primary outcome measure was the relative reduction in BP_{ND} (ΔBP_{ND}), reflecting amphetamine-induced dopamine release (i.e., dopamine release capacity).

For the purposes of a separate experiment, each subject received 2 post-amphetamine PET scans rather than only 1. For the current experiment we only used one of these scans, the one administered 5-7 hours post-amphetamine. Some subjects also had scans administered at 3 hours post-amphetamine and 10 hours post-amphetamine. We selected the 5-7 hour time point over the 3 hour time point as this was the time point with the most available data (15/18 subjects with data compared to 12/18 subjects for the 3 hour scan). The BP_{ND} for [^{11}C]raclopride in this study was found to be highly stable from the 3 hour time point to the 5-7 hour time point [86], so our selection of time point is highly unlikely to have any meaningful impact on the results.

MRI analysis

Voxel-based morphometry (VBM) analyses [91] on SPM12 included tissue segmentation, template generation, and normalization into MNI space using DARTEL routines [92], followed by spatial smoothing with an 8-mm^3 full-width-at-half-maximum Gaussian kernel. This created modulated maps of gray-matter "volume." Maps were scaled based on whole-brain gray-matter volume in the group-level analysis, which consisted of an ANCOVA incorporating a group factor (patients, controls) and the uncertainty adjustment, context mean effect, head coil type, and motion as covariates. Head coil type was included as a binary covariate because there were two subjects who were scanned with an 8-channel, rather than a 32-channel head coil. The presence of motion artifacts was also included as a binary covariate because there were 3 subjects whose T1 scan had minimal but visible motion artifacts.

A cluster-forming (height) threshold of $p \leq 0.005$ and extent threshold of 5 adjacent voxels was used. Clusters surviving a random-field-theory-based family-wise-error (FWE) correction at $p \leq 0.05$ were considered statistically significant.

Model description and simulations

We illustrate with simulations how a simple Bayesian model produces an uncertainty-dependent assimilation bias in Figure 1D, similar to prior work [83, 85, 93]. The model assumes that subjects estimate the true duration of the target tone (μ_{target}) as if it were drawn from a noisy, Gaussian distribution, from which context tone durations are also drawn. More specifically, we assume that subjects take the context tones to determine a prior for the true duration of the target tone. We take this prior to be normally distributed, with moments given by the maximum likelihood estimates (MLE) implied by the presented set of context tone durations. (For simplicity, we do not model the details of estimation of the prior itself. In particular, we do not account for subjects' additional uncertainty about the true mean and variance of the prior distribution owing to the context tones themselves being sampled. Also, although we assume objective persented durations are corrupted by perceptual timing noise, we do not explicitly model the consequent trial-by-trial variation in the moments of the prior. Instead, we account for it simply as contributing increased variance to the prior, and in trial-by-trial variation in the likelihood). The prior is then:

$$P(\mu_{target}) \sim N\left(\bar{x}_{context}, s^2_{context} + s^2_{sensory}\right),$$

where $\bar{x}_{context}$ is the actual context mean for the context tone durations used in the experiment, $s_{context}$ is the actual standard deviation of the context tone durations, and $s_{sensory}$ accounts for additional sensory noise associated with perception of tone durations over and above the actual programmed variation in the durations (set to $s_{sensory} = 70$ given that the coefficient of variation SD/mean in humans is ~0.1 for this range of durations [83, 85] and that the mean target duration is 700 ms). That is, we assume tones of true duration μ are perceived noisily with subjective duration $\bar{x}$, whose measurement distribution $P(\bar{x} \mid \mu)$ is given by a Gaussian with mean μ and SD $s_{sensory}$, and that this additional variance in perceived duration widens the prior distribution.

After listening to the target tone, the model assumes that subjects estimate the posterior probability of (or update their belief about) its true duration given this new observation using Bayes' rule as:

$$P\left(\mu_{target} \mid \bar{x}_{target}\right) \propto P(\bar{x}_{target} \mid \mu_{target}) \cdot P(\mu_{target}).$$

Here the likelihood function $P(\bar{x}_{target} \mid \mu_{target})$ is given by the measurement distribution, now viewed as a function of the unknown (to the subject) true duration μ_{target} given their (noisily) observed duration of the target tone, $\bar{x}_{target}$; this is also a Gaussian with mean $\bar{x}_{target}$ and SD $s_{sensory}$. Note that here, $\bar{x}_{target}$ denotes the subjectively perceived duration, which is assumed to fluctuate from trial to trial around the programmed target duration.

Thus, Bayesian cue combination is used here to optimally weigh the prior $P(\mu_{target})$ and the likelihood $P(\bar{x}_{target} \mid \mu_{target})$, based on the respective reliability or precision associated with these two sources of information (i.e., inversely proportional to their respective variance, $s^2_{context} + s^2_{sensory}$ and $s^2_{sensory}$) and yield a new estimate of the true duration of the target tone after listening to it, $P\left(\mu_{target} \mid \bar{x}_{target}\right)$. We model the subjects' perceived duration via the peak of this distribution (the maximum *a posteriori* [MAP] estimate), and assume that their reproduction durations, in turn, track these subjective estimates on average (perhaps corrupted by zero-mean motor noise). Note that because perceptual and production noise are zero-mean, the expected MAP estimate (and, in turn the mean reproduced interval), after marginalizing the subjectively measured $\bar{x}_{target}$ according to the measurement model and any production noise, is given by the MAP estimate for the case when $\bar{x}_{target}$ equals the true target duration (700 ms). This model thus naturally explains perceptual *assimilation* of the target tone toward the context mean and reduced assimilation under high-variance to low-variance contexts, which would correspond to a positive uncertainty adjustment in the VCTR task.

To simulate the neural deficit associated with hallucinations, in line with prior work [17] we assumed that a neural uncertainty signal $f(\sigma_{prior})$ encoding contextual uncertainty ($\sigma_{prior} = \sqrt{s^2_{context} + s^2_{sensory}}$) is a non-linear function that saturates at a maximum, specifically a rectified hyperbolic tangent function [94] of the form:

$$f(\sigma_{prior}) = max \cdot [\tanh(k \cdot \sigma_{prior})]_+$$

with slope k and maximum max. The severity of the deficit underlying hallucinations is assumed to result from a reduced range for neural encoding of uncertainty, i.e., on smaller maxima max in the function $f(\sigma_{prior})$. We propose that this could be due to a deficient downregulation of dopamine release in response to higher contextual uncertainty associated with the known excess of presynaptic synthesis and release of dopamine in psychosis. For the simulation, $f(\sigma_{prior})$, rather than σ_{prior}, is used in the Bayesian inference model to estimate the prior $P(\mu_{target})$ as $\sim N(\bar{x}_{context}, f(\sigma_{prior})^2)$, with decreasing values of max simulating more severe deficits. Simulations of this model suggest that more severe deficits in hallucinators result in reduced uncertainty adjustment in the VCTR task (Figure 1E), as the prior for high-variance contexts becomes more precise and thus closer to the prior for low-variance contexts under this deficit.